

Secrecy Analysis of Ambient Backscatter NOMA Systems under I/Q Imbalance

Xingwang Li, *Senior Member, IEEE*, Mengle Zhao, *Student Member, IEEE*, Yuanwei Liu, *Senior Member, IEEE*, Lihua Li, *Member, IEEE*, Zhiguo Ding, *Fellow, IEEE*, and Arumugam Nallanathan, *Fellow, IEEE*

Abstract—We investigate the reliability and security of the ambient backscatter (AmBC) non-orthogonal multiple access (NOMA) systems, where the source aims to communication with two NOMA users in the presence of an eavesdropper. We consider a more practical case that nodes and backscatter device (BD) suffer from in-phase and quadrature-phase imbalance (IQI). More specifically, exact analytical expressions for the outage probability (OP) and the intercept probability (IP) are derived in closed-form. Moreover, the asymptotic behaviors and corresponding diversity orders for the OP are discussed. Numerical results show that: 1) Although IQI reduces the reliability, it can enhance the security. 2) Compared with the traditional orthogonal multiple access (OMA) system, the AmBC-NOMA system can obtain better reliability when the signal-to-noise (SNR) ratio is low; 3) There are error floors for the OP because of the reflection coefficient β .

Index Terms—Ambient backscatter communication, in-phase and quadrature-phase imbalance, non-orthogonal multiple access, physical layer security

I. INTRODUCTION

Non-orthogonal multiple access (NOMA) has been identified as one of the key technologies of the fifth-generation (5G) mobile networks due since it has the advantages of high spectrum efficiency, massive connection and low latency [1]. Different from orthogonal multiple access (OMA), the dominant feature of NOMA is to ensure multiple users to occupy the the same frequency/time resources by power domain multiplexing. These advantages are achieved by employing superposed code (SC) at the transmitter and successive interference cancellation (SIC) at the receiver [2]. Moreover, NOMA can ensure the fairness by allocating more power to the weak users.

On a parallel avenue, ambient backscatter communication (AmBC) is known as a potential technology with high spectrum- and energy-efficient for the green Internet-of-Things (IoT) and has been attracted widespread attention in academia and industry [3]. In general, the AmBC system consists of three parts: ambient radio-frequency (RF) source, backscatter device (BD) and reader. In this respect, the cooperative AmBC

system was designed in [4] to allow the reader to recover information from both BD and RF source, and the analytical closed-form expressions for the bit error rate (BER) of the maximum-likelihood (ML), suboptimal linear detector and SIC detectors were derived. In [5], Guo *et al.* proposed a NOMA-assisted AmBC system to support massive BD connections.

Due to the broadcast characteristic of wireless environments, it is difficult to ensure secure communication for the wireless networks without being eavesdropped by the unauthored receivers. Physical layer security (PLS) has been known as an effective way to improve the security of communication systems, which has sparked a great deal of research interests [6–9]. The authors of [6] investigated the reliability and security of multi-relay networks in terms of the outage probability (OP) and the intercept probability (IP). Regarding NOMA systems, the authors proposed an enhanced security scheme to against full-duplex proactive eavesdropping [7]. To enhance the security of AmBC systems, the authors in [8] designed an optimal tag selection scheme of the multi-tag AmBC systems. However, the common characteristic of above works are assumed that the transceiver RF front-ends were equipped with ideal components. Unfortunately, the practical RF components are prone to in-phase and quadrature-phase imbalance (IQI) due to mismatch and manufacturing non-idealities [9], which limit the overall system performance. Therefore, it is of great practical significance to study the secrecy performance of the AmBC NOMA systems with IQI.

Although the PLS of the NOMA systems has been extensively studied, to the best of our knowledge, the impact of IQI on the PLS performance of the AmBC NOMA system has not yet been investigated. This work aims to bridge this gap and investigates the effects of IQI on the PLS of the AmBC NOMA systems, where the eavesdropper can intercept the signals from both the source and reflected signals from BD. Specifically, we study the reliability and security by deriving the analytical closed-form expressions of the OP and the IP for the far user, the near user and the BD, respectively. Furthermore, in order to obtain more insights, the asymptotic behavior for the OP at high signal-to-noise (SNR) is explored, as well as the diversity order. The results have shown that although IOI has deleterious effects on reliability, it can enhance the secure performance of the considered system. Moreover, the proposed AmBC system can provide highly secure communication for the BD.

II. SYSTEM MODEL

We consider a downlink AmBC NOMA system as illustrated in Fig. 1, which consists of one source S , one BD, one

X. Li and M. Zhao are with the School of Physics and Electronic Information Engineering, Henan Polytechnic University, Jiaozuo, China (email:lixingwangbupt@gmail.com, zhaomenglephu@163.com).

Y. Liu and A. Nallanathan are with the School of Electronic Engineering and Computer Science, Queen Mary University of London, London, UK, London, UK (email:{yuanwei.liu, a.nallanathan}@qmul.ac.uk).

L. Li is with the State Key Laboratory of Networking and Switching Technology, Beijing University of Posts and Telecommunications, China (email:lilihua@bupt.edu.cn).

Z. Ding is with the School of Electrical and Electronic Engineering, The University of Manchester, Manchester, UK (email:zhiguo.ding@manchester.ac.uk).

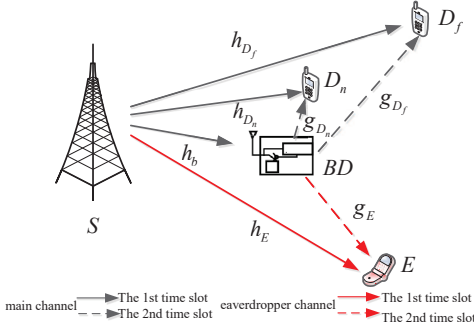


Fig. 1. System model

far user (D_f), one near user (D_n) and one eavesdropper (E). We assume that: i) All the nodes are equipped with a single antenna; ii) The transceiver RF front-ends of the all nodes suffer from IQI. For convenience, we have $h_i \sim \mathcal{CN}(0, \lambda_k)$, $g_i \sim \mathcal{CN}(0, \lambda_k)$, $i \in \{D_n, D_f, E\}$, $k \in \{1, 2, 3, 4, 5, 6\}$ and $h_b \sim \mathcal{CN}(0, \lambda_7)$,

As in [9], IQI is modeled as phase and/or amplitude imbalance between the in-phase (I) and quadrature-phase (Q) branches. Thus, the time-domain baseband TX signals with IQI at S can be expressed as

$$y_s = \mu_{t_s} x_s + \nu_{t_s} (x_s)^*, \quad (1)$$

where $x_s = \sqrt{a_1 P_s} x_1 + \sqrt{a_2 P_s} x_2$, P_s is the transmit power at S ; a_1 and a_2 are the power allocation coefficients with $a_1 + a_2 = 1$ and $a_1 < a_2$, respectively; x_1 and x_2 are corresponding transmitted signals of D_f and D_n with $E(|x_1|^2) = E(|x_2|^2) = 1$, where $E(\cdot)$ and $(\cdot)^*$ are the expectation and conjugation operations, respectively. Moreover, $\mu_{t_s} = \frac{1}{2}(1 + \varsigma_t \exp(j\phi_t))$, $\nu_{t_s} = \frac{1}{2}(1 - \varsigma_t \exp(-j\phi_t))$, where ς_t and ϕ_t denote the TX amplitude and phase mismatch levels, respectively.

The BD backscatters the received signal to D_n with its own signal $c(t)$ with $E(|c(t)|^2) = 1$. Two types of received signals at i are transmitted from S and backscattered from BD. Considering IQI at transceivers, the received signals at i are given by

$$y_i = \mu_{r_i} \{ \beta y_{BD} g_i [\mu_{t_{BD}} c(t) + \nu_{t_{BD}} (c(t))^*] + h_i y_s + n_i \} + \nu_{r_i} \{ \beta y_{BD} g_i [\mu_{t_{BD}} c(t) + \nu_{t_{BD}} (c(t))^*] + h_i y_s + n_i \}^*, \quad (2)$$

where β is a complex reflection coefficient used to normalize $c(t)$; $n_i \sim \mathcal{CN}(0, N_0)$ is the complex additive white Gaussian noise (AWGN); h_i and g_i are the channel coefficients $S \rightarrow i$ and $BD \rightarrow i$, respectively. Moreover, $\mu_{r_i} = \frac{1}{2}(1 + \varsigma_{r_i} \exp(-j\phi_{r_i}))$, $\nu_{r_i} = \frac{1}{2}(1 - \varsigma_{r_i} \exp(j\phi_{r_i}))$, where ς_{r_i} and ϕ_{r_i} are the RX amplitude and phase mismatch levels, respectively. $y_{BD} = \mu_{r_{BD}} h_b y_s + \nu_{r_{BD}} (h_b y_s)^*$ is the received signals at BD, where h_b is the channel coefficient of $S \rightarrow BD$. The received signal-to-interference-plus-noise ratio (SINR) for D_f to decode the signal x_2 can be obtained as

$$\gamma_{D_f}^{x_2} = \frac{\xi_{D_f} a_2 \rho_{D_f} \gamma}{\rho_{g_{D_f}} \rho_b (A_{D_f} + Q_{D_f}) \gamma + \rho_{D_f} C_{D_f} \gamma + D_{D_f}}, \quad (3)$$

According to the NOMA principle, D_n and E can decode signal x_2 , x_1 , and $c(t)$ in turn with the aid of SIC. Then, the received SINR of i can be given as

$$\gamma_i^{x_2} = \frac{\xi_i a_2 \rho_{D_n} \gamma}{\rho_{g_i} \rho_b (A_i + Q_i) \gamma + \rho_i C_i \gamma + D_i}, \quad (4)$$

$$\gamma_i^{x_1} = \frac{\xi_i a_1 \rho_i \gamma}{\rho_{g_i} \rho_b (A_i + Q_i) \gamma + \rho_i (a_2 B_i + M_i) \gamma + D_i}, \quad (5)$$

$$\gamma_i^{c(t)} = \frac{Q_i \rho_{g_i} \rho_b \gamma}{\rho_{g_i} \rho_b A_i \gamma + \rho_i (B_i + M_i) \gamma + D_i}, \quad (6)$$

where $\gamma = P_s/N_0$ represents the transmit SNR at S ; $\rho_i = |h_i|^2$, $\rho_{g_i} = |g_i|^2$, $\rho_b = |h_b|^2$, $A_i = |\mu_{r_i}|^2 \beta^2 |\mu_{r_{BD}}|^2 |\nu_{t_{BD}}|^2 (|\mu_{t_s}|^2 + |\nu_{t_s}|^2) + |\mu_{r_i}|^2 \beta^2 |\nu_{r_{BD}}|^2 \times |\nu_{t_{BD}}|^2 (|\mu_{t_s}^*|^2 + |\nu_{t_s}^*|^2) + |\nu_{r_i}|^2 \beta^2 |\mu_{r_{BD}}^*|^2 |\mu_{t_{BD}}^*|^2 \times (|\mu_{t_s}^*|^2 + |\nu_{t_s}^*|^2) + |\nu_{r_i}|^2 \beta^2 |\nu_{r_{BD}}^*|^2 |\mu_{t_{BD}}^*|^2 (|\mu_{t_s}|^2 + |\nu_{t_s}|^2)$, $Q_i = |\mu_{r_i}|^2 \beta^2 |\mu_{r_{BD}}|^2 |\mu_{t_{BD}}|^2 (|\mu_{t_s}|^2 + |\nu_{t_s}|^2) + |\mu_{r_i}|^2 \beta^2 |\nu_{r_{BD}}|^2 \times |\mu_{t_{BD}}|^2 (|\mu_{t_s}^*|^2 + |\nu_{t_s}^*|^2) + |\nu_{r_i}|^2 \beta^2 |\mu_{r_{BD}}^*|^2 |\nu_{t_{BD}}^*|^2 \times (|\mu_{t_s}^*|^2 + |\nu_{t_s}^*|^2) + |\nu_{r_i}|^2 \beta^2 |\nu_{r_{BD}}^*|^2 |\nu_{t_{BD}}^*|^2 (|\mu_{t_s}|^2 + |\nu_{t_s}|^2)$, $\xi_i = |\mu_{r_i}|^2 |\mu_{t_s}|^2 + |\nu_{r_i}|^2 |\nu_{t_s}^*|^2$, $B_i = |\mu_{r_i} \mu_{t_s} - 1|^2 + |\nu_{r_i}|^2 |\nu_{t_s}^*|^2$, $C_i = a_1 \xi_i + M_i$, $D_i = |\mu_{r_i}|^2 + |\nu_{r_i}|^2$, $M_i = |\mu_{r_i}|^2 |\nu_{t_s}|^2 + |\nu_{r_i}|^2 |\mu_{t_s}^*|^2$.

III. PERFORMANCE ANALYSES

This section evaluates the reliability and security of the AmBC NOMA systems by deriving the analytical expressions for the OP and the IP.¹ Moreover, we examine asymptotic outage behavior and the diversity order in the high SNR region.

A. Outage Probability Analysis

1) Outage Probability for D_f

According to NOMA principle, the outage event occurs at D_f when D_f cannot successfully decode x_2 . Thus, the OP at D_f can be represented as

$$P_{out}^{D_f} = 1 - \text{Pr}(\gamma_{D_f}^{x_2} > \gamma_{th2}), \quad (7)$$

where γ_{th2} is the target rate at D_f .

Theorem 1. For Rayleigh fading channels, the analytical expression for the OP of the far user can be obtained as²

$$P_{out}^{D_f} = 1 + \Delta_1 e^{\Delta_1} \text{Ei}(-\Delta_1), \quad (8)$$

where $A_1 = \gamma_{th2} / (\xi_{D_f} a_2 - C_{D_f} \gamma_{th2})$, $\Delta_1 = \lambda_2 / (\lambda_7 \lambda_5 A_1 (A_{D_f} + Q_{D_f}))$, and $\text{Ei}(x) = \int_{-\infty}^x \frac{e^{\rho}}{\rho} d\rho$ is the exponential integral function [11].

¹The reliability and security are another metrics to characterize the PLS of wireless communication systems without using any secrecy coding, which are formulated by the OP and the IP [10].

²The ideal and non-ideal results of OP and IP for the far user and near user can be written in an unified expression in (8), (10), (12), (13), (23) and (24).

Proof. By substituting (3) into (10), the OP of D_f can be expressed as

$$P_{out}^{D_f} = \int_{A_1}^{\infty} \left(\rho_{g_{D_f}} \rho_b(A_{D_f} + Q_{D_f}) + D_{D_f} \right) f_{\rho_{D_f}} \int_0^{\infty} f_{\rho_{g_{D_f}}} \rho_b(y) dx dy$$

$$= \frac{2}{\lambda_7 \lambda_5} \int_0^{\infty} e^{-\frac{A_1 [y(A_{D_f} + Q_{D_f}) + D_{D_f}]}{\lambda_2}} K_0 \left(2 \sqrt{\frac{y}{\lambda_7 \lambda_5}} \right) dy, \quad (9)$$

where $f_{\rho_{D_f}} = \frac{1}{\lambda_2} e^{-\frac{x}{\lambda_2}}$, $f_{\rho_{g_{D_f}}} \rho_b(y) = \frac{2K_0 \left(2 \sqrt{\frac{y}{\lambda_7 \lambda_5}} \right)}{\lambda_7 \lambda_5}$, $K_0(x)$ is the modified Bessel function of the second kind. By using the integral equation [11, Eq. (6.614)], we can obtain (11) after some mathematical manipulations. \square

Corollary 1. *At high SNRs, the asymptotic expression for the OP of D_f of the AmBC NOMA system is given as*

$$P_{out,\infty}^{\Delta_1} = 1 + \Delta_1 e^{\Delta_1} \text{Ei}(-\Delta_1), \quad (10)$$

2) Outage Probability for D_n

To successfully decode x_1 at D_n , two conditions are needed to be met: 1) D_n can successfully decode x_2 ; 2) D_n can successfully decode its own information x_1 . Therefore, the OP of D_n can be expressed as

$$P_{out}^{D_n} = 1 - \text{Pr} \left(\gamma_{D_n}^{x_2} > \gamma_{th2}, \gamma_{D_n}^{x_1} > \gamma_{th1} \right), \quad (11)$$

where γ_{th1} is the target rate at D_n .

Theorem 2. *For Rayleigh fading channels, the analytical expression for OP of the near user can be obtained as*

$$P_{out}^{D_n} = 1 + \Delta_2 e^{\Delta_2 - \frac{\varsigma D_{D_n}}{\lambda_1 \gamma}} \text{Ei}(-\Delta_2), \quad (12)$$

where $\varsigma = \max \left\{ \frac{\gamma_{th1}}{\xi_{D_n} a_1 - (a_2 B_{D_n} + M_{D_n}) \gamma_{th1}}, \frac{\gamma_{th2}}{\xi_{D_n} a_2 - C_{D_n} \gamma_{th2}} \right\}$, $\Delta_2 = \frac{\lambda_1}{\lambda_7 \lambda_4 (A_{D_n} + Q_{D_n})}$.

Proof. Following the similar derivation process of $P_{out}^{D_f}$, by substituting (4), (5) into (14), we can obtain $P_{out}^{D_n}$. \square

Corollary 2. *At high SNRs, the asymptotic expression for the OP of D_f of the AmBC NOMA system is given as*

$$P_{out,\infty}^{D_n} = 1 + \Delta_2 e^{\Delta_2} \text{Ei}(-\Delta_2), \quad (13)$$

3) Outage Probability for BD

The BD signals can be successfully decoded when x_2 and x_1 are perfectly decode at D_n . Thus, the OP of BD can be expressed as

$$P_{out}^{BD} = 1 - \text{Pr} \left(\gamma_{D_n}^{x_2} > \gamma_{th2}, \gamma_{D_n}^{x_1} > \gamma_{th1}, \gamma_{D_n}^{c(t)} > \gamma_{thc} \right), \quad (14)$$

where γ_{thc} is the target rate for decoding BD signals.

Theorem 3. *For Rayleigh fading channels, we have*

- *Ideal conditions* ($\varsigma_t = \varsigma_r = 1$, $\phi_t = \phi_r = 0^\circ$)

For ideal conditions, the analytical expression for the OP of the BD in (15) is at the top of next page.

where $\varsigma_{id} = \max \left\{ \frac{\gamma_{th2}}{a_2 - a_1 \gamma_{th2}}, \frac{\gamma_{th1}}{a_1} \right\}$, $\Delta_3 = \frac{\lambda_1}{\lambda_7 \lambda_4 \varsigma_{id} \beta^2}$, $\vartheta_k = \cos \left[\frac{(2k-1)\pi}{2N} \right]$, N is an accuracy-complexity tradeoff parameter.

- *Non-ideal conditions*

For Non-ideal conditions, the analytical expression for the OP of BD in (16) is at the top of next page.

where $\Delta_4 = \frac{\lambda_1 (B_{D_n} + M_{D_n}) \gamma_{thc}}{\lambda_7 \lambda_4 (Q_{D_n} - A_{D_n} \gamma_{thc})}$, $\Delta_5 = \frac{\lambda_1}{\lambda_7 \lambda_4 \varsigma (A_{D_n} + Q_{D_n})}$, $\Delta_6 = \frac{D_{D_n} \gamma_{thc}}{(Q_{D_n} \gamma - A_{D_n} \gamma_{thc})}$, $\Delta_7 = 2 \sqrt{\frac{(\vartheta_k + 1) R_6}{2 \lambda_7 \lambda_4}}$, $\Delta_8 = \frac{\varsigma (A_{D_n} + Q_{D_n}) (\vartheta_k + 1) R_6}{2 \lambda_1 \gamma}$.

Proof. For ideal conditions, substituting $\varsigma_t = \varsigma_r = 1$ and $\phi_t = \phi_r = 0^\circ$ into (4), (5), (6), then according to (14), $P_{out}^{BD,id}$ can be expressed as

$$P_{out}^{BD,id} = \int_{\frac{\gamma_{thc}}{\beta^2 \gamma}}^{\infty} e^{-\frac{\varsigma_{id} (y \beta^2 + 1)}{\lambda_1}} \frac{2}{\lambda_7 \lambda_4} K_0 \left(2 \sqrt{\frac{y}{\lambda_7 \lambda_4}} \right) dy$$

$$= \int_0^{\infty} e^{-\frac{\varsigma_{id} (y \beta^2 + 1)}{\lambda_1}} \frac{2}{\lambda_7 \lambda_4} K_0 \left(2 \sqrt{\frac{y}{\lambda_7 \lambda_4}} \right) dy$$

$$- \underbrace{\int_0^{\frac{\gamma_{thc}}{\beta^2 \gamma}} e^{-\frac{\varsigma_{id} (y \beta^2 + 1)}{\lambda_1}} \frac{2}{\lambda_7 \lambda_4} K_0 \left(2 \sqrt{\frac{y}{\lambda_7 \lambda_4}} \right) dy}_a, \quad (17)$$

where a can be approximated by Gaussian-Chebyshev quadrature [12]. Utilizing [11, Eq. (6.611)] to the first term of (17), we can obtain the result of (18) after some mathematical manipulations. Similarly, $P_{out}^{BD,ni}$ can be obtained. \square

Corollary 3. *At high SNRs, the asymptotic expressions for the OP of BD for the AmBC NOMA system can be given by*

- *Ideal conditions*

$$P_{out,\infty}^{BD,id} = 1 + \Delta_3 e^{\Delta_3} \text{Ei}(-\Delta_3), \quad (18)$$

- *Non-ideal conditions*

$$P_{out,\infty}^{BD,mi} = 1 - \Delta_4 e^{\Delta_4} \text{Ei}(-\Delta_4) + \Delta_5 e^{\Delta_5} \text{Ei}(-\Delta_5). \quad (19)$$

Furthermore, the diversity order is investigated, which can be defined as:

$$d = - \lim_{\gamma \rightarrow \infty} \frac{\log(P_{out}^{\infty})}{\log \gamma}, \quad (20)$$

Corollary 4. *The diversity order of D_f , D_n and BD are given as:*

$$d_{D_f} = d_{D_n} = d_{BD}^{id} = d_{BD}^{ni}. \quad (21)$$

Remark 1. *From Corollary 1, Corollary 2, Corollary 3 and Corollary 4, we can see that when transmit SNR goes to infinity, the asymptotic outage performance of the D_f , D_n and BD become a constant. It means that the OP exists error floor, which results in 0 diversity order. This error floor is determined by the parameters of IQI and the reflection coefficient β .*

B. Intercept Probability Analysis

User j , $j \in \{D_f, D_n, BD\}$ will be intercepted if E can successfully wiretap j 's signal, i.e. $\gamma_E^p > \gamma_{thE,j}$, $p \in \{x_2, x_1, c(t)\}$. Thus, the IP of j by E can be expressed as

$$P_{int}^j = \text{Pr} \left(\gamma_E^p > \gamma_{thE,j} \right), \quad (22)$$

where $\gamma_{thE,j}$ is the secrecy SNR threshold for j .

Theorem 4. *For Rayleigh fading channels, the analytical expressions for the IP of the far user, the near user and BD can be respectively obtained as*

$$P_{out}^{BD,id} = 1 + \Delta_3 e^{\Delta_3 - \frac{\varsigma_{id}}{\gamma \lambda_1}} \text{Ei}(-\Delta_3) + \frac{\pi \gamma_{thc}}{N \beta^2 \gamma \lambda_7 \lambda_4} e^{-\frac{\varsigma_{id}}{\gamma \lambda_1}} \sum_{k=0}^N e^{-\frac{\gamma_{thc}(\vartheta_k+1)}{2\lambda_1}} K_0 \left(2 \sqrt{\frac{\gamma_{thc}(\vartheta_k+1)}{2\beta^2 \gamma \lambda_7 \lambda_4}} \right) \sqrt{1 - \vartheta_k^2}, \quad (15)$$

$$P_{out}^{BD,ni} = 1 - \Delta_4 e^{\frac{D_{D_n}}{\lambda_1(B_{D_n}+M_{D_n})\gamma} + \Delta_4} \text{Ei}(-\Delta_4) + \Delta_5 e^{\Delta_5 - \frac{\varsigma_{D_n}}{\gamma \lambda_1}} \text{Ei}(-\Delta_5) + e^{-\frac{\varsigma_{D_n}}{\gamma \lambda_1}} \frac{\pi \Delta_6}{N \lambda_3 \lambda_5} \sum_{k=0}^N e^{-\Delta_8} K_0(\Delta_7) \sqrt{1 - \vartheta_k^2} \\ - e^{\frac{D_{D_n}}{\lambda_1(B_{D_n}+M_{D_n})\gamma}} \frac{\pi \Delta_6}{N \lambda_7 \lambda_4} \sum_{k=0}^N e^{-\frac{D_{D_n}(\vartheta_k+1)}{2\lambda_1(B_{D_n}+M_{D_n})\gamma}} K_0(\Delta_7) \sqrt{1 - \vartheta_k^2}, \quad (16)$$

For the far user and near user, we have

$$P_{int}^{D_f} = -\Delta_9 e^{\Delta_9 - \frac{D_{E,A_2}}{\lambda_2}} \text{Ei}(-\Delta_9), \quad (23)$$

$$P_{int}^{D_n} = -\Delta_{10} e^{\frac{\Delta_{10} - \frac{D_{E\gamma_{thE1}}}{\lambda_3(|\mu_{rE}|^2 |\mu_{tE}|^2 a_1 \gamma - (a_2 B_E + M_E) \gamma \gamma_{thE1})}}{\lambda_3(|\mu_{rE}|^2 |\mu_{tE}|^2 a_1 \gamma - (a_2 B_E + M_E) \gamma \gamma_{thE1})}} \text{Ei}(-\Delta_{10}), \quad (24)$$

$$\text{where } \Delta_9 = \frac{\lambda_4}{\lambda_7 \lambda_6 A_2 (A_E + Q_E)}, \quad A_2 = \frac{\gamma_{thE2}}{\xi_E a_2 - C_E \gamma_{thE2}}, \quad \Delta_{10} = \frac{\lambda_3(|\mu_{rE}|^2 |\mu_{tE}|^2 a_1 \gamma - (a_2 B_E + M_E) \gamma \gamma_{thE1})}{\lambda_7 \lambda_6 (A_E + Q_E) \gamma_{thE1}}.$$

For the BD, we have

- *Ideal conditions* ($\varsigma_t = \varsigma_r = 1$, $\phi_t = \phi_r = 0^\circ$)

$$P_{int}^{BD,id} = 1 - \frac{\pi \gamma_{thE3}}{N \lambda_7 \lambda_6 \beta^2 \gamma} \sum_{k=0}^N K_0 \left(2 \sqrt{\frac{\gamma_{thE3}(\vartheta_k+1)}{2\lambda_7 \lambda_6 \beta^2 \gamma}} \right) \sqrt{1 - \vartheta_k^2}, \quad (25)$$

- *Non-ideal conditions*

For Non-ideal conditions, the analytical expression for the IP of BD in (26) is at the top of next page.

$$\text{where } \Delta_{11} = \frac{D_{E\gamma_{thE3}}}{\lambda_7 \lambda_6 (Q_E \gamma - A_E \gamma \gamma_{thE3})}, \quad \Delta_{12} = \frac{\lambda_3(B_E + M_E) \gamma_{thE3}}{\lambda_7 \lambda_6 (Q_E - A_E \gamma_{thE3})}, \quad \Delta_{13} = 2 \sqrt{\frac{\Delta_{11}(\vartheta_k+1)}{2}}.$$

Remark 2. From Theorem 4, We can obtain that as the reflection coefficient β increases, $P_{int}^{D_f}$ and $P_{int}^{D_n}$ decreases, while P_{int}^{BD} increases; Moreover, IQI parameters has a beneficial effect on the IPs for the far user, the near user and the BD.

IV. NUMERICAL RESULTS

This section provides some numerical results to validate the correctness of the analysis in Section III. The results are verified by using Monte Carlo simulations with 10^6 trials. Unless otherwise stated, we have the following settings: $N_0 = 1$, $\gamma_{thf} = 1$, $\gamma_{thn} = 2$, $\gamma_{thc} = 0.1$, $\gamma_{thE,D_n} = 1$, $\gamma_{thE,D_f} = 1.2$, $\gamma_{thE,BD} = 0.8$; The power allocation coefficients are $a_1 = 0.1$ and $a_2 = 0.9$; The channel fading parameters are $\lambda_1 = \lambda_3 = 1$, $\lambda_2 = 0.1$, $\lambda_4 = 0.5$, $\lambda_5 = 0.8$, $\lambda_6 = 0.2$, $\lambda_7 = 0.1$. The reflection coefficient is $\beta = 0.1$, while for the ideal RF front-end, $\varsigma_t = \varsigma_r = 1$, $\phi_t = \phi_r = 0$.

Fig. 2 plots the OP and IP versus transmit SNR under ideal and IQI conditions with $\varsigma_t = \varsigma_r = 1.05$, $\phi_t = \phi_r = 20^\circ$. The theoretical results are in excellent agreement with the equivalent simulated results. A specific observation can be obtained that IQI have significant effect on the near user, this happens because that the near user suffers from SIC, which

is impaired by IQI. The changes of OP and IP for BD are very obvious due to the effects of two time SIC impaired by IQI, which indicate that BD performance is more sensitive to IQI at high SNRs. On the other hand, although IQI reduces the reliability of the considered system, it enhances the security to some extent. Finally, we can also see that there exists a trade-off between reliability and security, that is, when the outage performance is relaxed, IP can be enhanced, and vice versa.

Fig. 3 demonstrates the impact of IP versus OP under ideal/non-ideal conditions $\varsigma_t = \varsigma_r = \{1, 1.05\}$, $\phi_t = \phi_r = \{0^\circ, 25^\circ\}$. For the purpose of comparison, the curves of OMA are provided with $\gamma_{thc}^{OMA} = \gamma_{thE,BD}^{OMA} = 1.8$.³ These results show that for a given OP, as IQI increases the corresponding IP reduces, which leads the decrease of the secrecy performance. In addition, we can observe that the effect of IQI on each user is different. This effect depends on the decoding order of the users and the system parameter settings, in which the far user is the least affected and experiences almost no performance degradation caused by the presence of IQI. BD changes is most significant. We can also observe that for a given OP, the secure performance of NOMA is better than that of OMA system for the near user, the performance of the far user is the opposite, this is due to the large power allocation parameter of the far user. Finally, it should be noted that the IP of the BD is the smallest, i.e., the BD has the best secure performance.

Fig.4 presents the OP and IP versus the reflection coefficient β for different power allocation parameter a_1 with $\varsigma_t = \varsigma_r = 1.1$, $\phi_t = \phi_r = 5^\circ$, where the transmit SNR for OP and IP are $SNR = 25dB$, $SNR = 10dB$. From these curves, we can observe that $P_{out}^{D_f}$ and $P_{out}^{D_n}$ increases, $P_{int}^{D_f}$ and $P_{int}^{D_n}$ decrease with the increase of β . This happens because that when β becomes large, the interference of the backscatter link increases, which reduces the reliability of D_f and D_n , and improve the security. The OP of BD decreases first and then increases as β increases. This happens because that when β is small, it is easier for D_n to decode its own information successfully, but it is difficult to decode BD signals. When β is large, it is difficult for D_n to decode its own information successfully. Noted that when $SNR = 25dB$, the outage performance is optimal when $\beta = 0.14$ for $a_1 = 0.2$, $\beta = 0.12$

³The reason for this parameter setting is that when the parameter of NOMA is set to $\gamma_{thc}^{OMA} = \gamma_{thE,BD}^{OMA} = 1.8$, which lead to the OP of BD is 1, and the IP is too small.

$$\begin{aligned}
P_{out}^{BD,ni} = & 1 - \frac{\pi\Delta_{11}}{N} \sum_{k=0}^N K_0(\Delta_{13}) \sqrt{1 - \vartheta_k^2} + \Delta_{12} e^{\frac{D_E}{\lambda_3(B_E+M_E)\gamma} + \Delta_{12}} \text{Ei}(-\Delta_{12}) \\
& + e^{\frac{D_E}{\lambda_3(B_E+M_E)\gamma}} \frac{\pi\Delta_{11}}{N} \sum_{k=0}^N e^{-\frac{D_E(\vartheta_k+1)}{2\lambda_3(B_E+M_E)\gamma}} K_0(\Delta_{13}) \sqrt{1 - \vartheta_k^2},
\end{aligned} \quad (26)$$

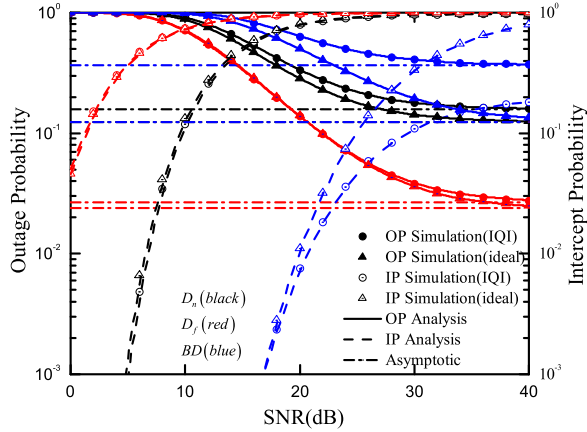


Fig. 2. OP and IP versus the transmit SNR

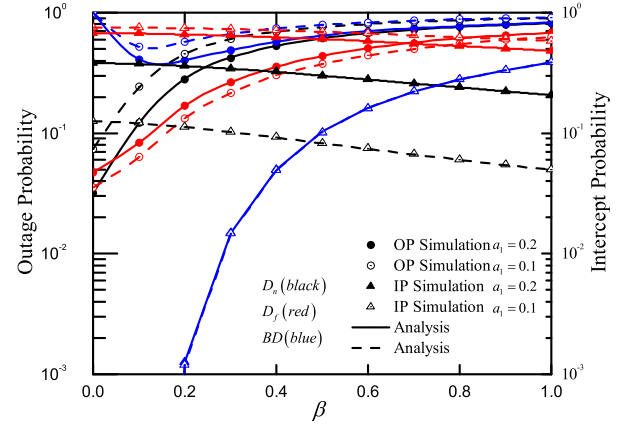


Fig. 4. OP and IP versus the reflection coefficient β for different power allocation parameter a_1

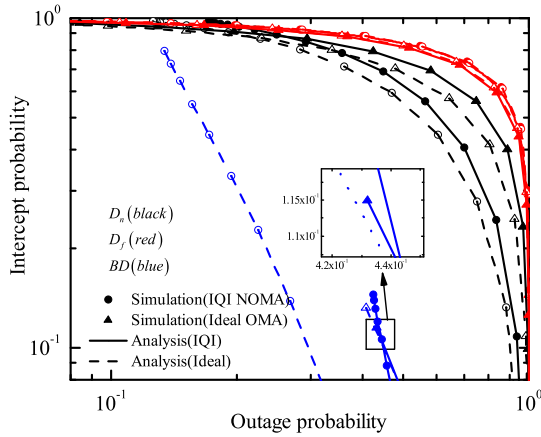


Fig. 3. IP versus OP for the D_f , D_n and BD

for $a_1 = 0.1$. This means that the optimal reflection coefficient is determined by power allocation coefficient.

V. CONCLUSION

This paper investigates the impact of IQI on the reliability and security of the AmBC NOMA system. This is carried out by deriving closed-form analytical expressions of the OP and IP in the presence of IQI, and the asymptotic behavior in the high SNR regime and diversity order for the OP are analyzed. The simulation results show that although IQI reduces the reliability for the far user, the near user and the BD, while it also improves the security of the three devices. In addition,

the increase of β will increase the OP and decrease the IP for far user and near user. Finally, we can conclude that BD of the AmBC NOMA system has better secrecy performance, which drives the application in the IoT networks.

REFERENCES

- [1] Y. Li, M. Jiang, Q. Zhang, Q. Li, and J. Qin, "Cooperative Non-Orthogonal Multiple Access in Multiple-Input-Multiple-Output Channels," *IEEE Trans. Wireless Commun.*, vol. 17, no. 3, pp. 2068–2079, March 2018.
- [2] X. Li, J. Li, Y. Liu, Z. Ding, and A. Nallanathan, "Residual Transceiver Hardware Impairments on Cooperative NOMA Networks," *IEEE Trans. Wireless Commun.*, vol. 19, no. 1, pp. 680–695, Jan 2020.
- [3] V. Liu, A. Parks, V. Talla, S. Gollakota, D. Wetherall, and J. R. Smith, "Ambient Backscatter: Wireless Communication out of Thin Air," *ACM SIGCOMM*, vol. 43, no. 4, pp. 39–50, Aug 2013.
- [4] G. Yang, Q. Zhang, and Y. Liang, "Cooperative Ambient Backscatter Communications for Green Internet-of-Things," *IEEE Internet Things J.*, vol. 5, no. 2, pp. 1116–1130, April 2018.
- [5] J. Guo, X. Zhou, S. Durrani, and H. Yanikomeroglu, "Design of Non-Orthogonal Multiple Access Enhanced Backscatter Communication," *IEEE Trans. Wireless Commun.*, vol. 17, no. 10, pp. 6837–6852, Oct 2018.
- [6] X. Li, M. Huang, C. Zhang, D. Deng, K. M. Rabie, Y. Ding, and J. Du, "Security and reliability performance analysis of cooperative multi-relay systems with nonlinear energy harvesters and hardware impairments," *IEEE Access*, vol. 7, pp. 102 644–102 661, 2019.
- [7] L. Lv, Z. Ding, J. Chen, and N. Al-Dhahir, "Design of Secure NOMA Against Full-Duplex Proactive Eavesdropping," *IEEE Wireless Commun. Lett.*, vol. 8, no. 4, pp. 1090–1094, Aug 2019.
- [8] Y. Zhang, F. Gao, L. Fan, X. Lei, and G. K. Karagiannidis, "Secure Communications for Multi-Tag Backscatter Systems," *IEEE Wireless Commun. Lett.*, vol. 8, no. 4, pp. 1146–1149, Aug 2019.
- [9] X. Li, M. Liu, C. Deng, P. T. Mathiopoulos, Z. Ding, and Y. Liu, "Full-Duplex cooperative NOMA Relaying Systems With I/Q Imbalance and Imperfect SIC," *IEEE Wireless Commun. Lett.*, vol. 9, no. 1, pp. 17–20, Jan 2020.

- [10] Y. Zou, J. Zhu, X. Li, and L. Hanzo, "Relay selection for wireless communications against eavesdropping: a security-reliability trade-off perspective," *IEEE Network*, vol. 30, no. 5, pp. 74–79, Sep. 2016.
- [11] I. S. Gradshteyn and I. M. Ryzhik, *Table of Integrals, Series, and Products*. New York, NY, USA: Academic, 2014.
- [12] F. B. Hildebrand, *Introduction to numerical analysis*. New York, USA: Dover Publications, 1987.